J. Fluid Mech. (2019), *vol.* 866, *pp.* 431–449.
doi:10.1017/jfm.2019.57

The Basset problem with dynamic slip: slip-induced memory effect and slip–stick transition

A. R. Premlata[1] **and Hsien-Hung Wei**[1,†]

[1]Department of Chemical Engineering, National Cheng Kung University, Tainan 701, Taiwan

(Received 5 November 2018; revised 25 December 2018; accepted 11 January 2019; first published online 13 March 2019)

When there exists slip on the surface of a solid body moving in an unsteady manner, the extent of slip is not fixed but constantly changes with the time-varying Stokes boundary layer thickness δ in competition with the slip length λ. Here we revisit the unsteady motion of a slippery spherical particle to elucidate this dynamic slip situation. We find that even if the amount of slip is minuscule, it can dramatically change the characteristics of the history force, markedly different from those due to non-spherical and fluid particles (Lawrence & Weinbaum, *J. Fluid Mech.*, vol. 171, 1986, pp. 209–218; Yang & Leal, *Phys. Fluids* A, vol. 3, 1991, pp. 1822–1824). For an oscillatory translation of such a particle of radius a, two distinctive features are identified in the frequency response of the viscous drag: (i) the high-frequency constant force plateau of $O(a/\lambda)$ much greater than the steady drag due to a constant shear stress caused by δ much thinner than λ and (ii) the persistence of the plateau while lowering the frequency until the slip–stick transition point $\delta \sim \lambda$, beyond which δ becomes thicker and the usual Basset decay reappears. Similar features can also be observed in the short-term force response for the particle subject to a sudden movement, as well as in the behaviour of the torque when it undergoes rotary oscillations. In addition, for both translational and rotary oscillations, slip can further introduce a phase jump from the no-slip value to zero in the high-frequency limit. As these features and the associated slip–stick transitions become more evident as λ becomes smaller and are exclusive to the situation where surface slip is present, they might have potential uses for extracting the slip length of a colloidal particle from experiments.

Key words: low-Reynolds-number flows

1. Introduction

Since Basset (1888) solved the time-dependent motion of a rigid sphere under the creeping flow condition, many extensions or variants have been performed along similar lines. Bentwich & Miloh (1978) derived a matched Stokes–Oseen solution for an unsteady flow past a sphere. Lawrence & Weinbaum (1986, 1988) obtained the force acting on an axisymmetric body in an unsteady motion. Pozrikidis (1989) developed a singularity method to construct a solution for unsteady Stokes flow

† Email address for correspondence: hhwei@mail.ncku.edu.tw

and confirmed the result obtained by Lawrence & Weinbaum (1988). The force characteristics for unsteady motions of fluid particles were examined by Kim & Karrila (1991) and Yang & Leal (1991). Their results were later corrected by Galindo & Gerbeth (1993). Lovalenti & Brady (1993) provided a unified account of the forces on a rigid particle, drop and bubble in arbitrary time-dependent motion at small Reynolds number. Feng & Joseph (1995) carried out direct numerical simulations to examine the validity of the quasi-steady approach for solving unsteady viscous flows around freely moving particles. Zhang & Stone (1998) derived dual integral equations to solve for oscillatory motions of circular discs. They were able to reveal detailed force characteristics by solving the equations analytically. Recently, Wang & Ardekani (2012) analysed an unsteady self-swimming squirmer and found that its propulsion can be generated by unsteady inertial effects. Simha, Mo & Morrison (2018) looked at unsteady Stokes flow near boundaries and provided a thorough analysis for the validity of the point-particle approximation.

Like the studies mentioned above, most of the existing investigations of unsteady Stokes flow are based on the no-slip boundary condition. If slip is allowed on the surface of a particle, only a few studies have addressed how slip influences the unsteady hydrodynamic responses (Albano, Bedeaux & Mazur 1975; Felderhof 1976; Michaelides & Feng 1995; Gatignol 2007; Ashmawy 2012, 2017). In these studies the expressions for the force and torque were derived, including the no-slip and the stress-free results as the limiting cases.

From a physical standpoint, one might think that the inclusion of surface slip is a trivial extension because it does nothing but drag reduction. In this work, we will show that this is not the case, and new features can be introduced through slip effects.

Compared to its steady counterpart, aside from the added mass term which is purely of the potential-flow origin, perhaps the most distinctive feature of an unsteady Stokes flow is the existence of the Basset history force that accounts for memory effects on the hydrodynamic force on a sphere. Lawrence & Weinbaum (1986) showed in their study of the unsteady force on an arbitrary axisymmetric body that a new memory term can emerge when the body is non-spherical. The memory kernel they found actually takes the form of $\exp(\alpha^2 t)\mathrm{erfc}(\alpha t^{1/2})$ which is finite as $t \to 0$, in contrast to the $t^{-1/2}$ form for the Basset kernel, where t is time and α is a parameter. However, Yang & Leal (1991) found that this new memory term can also exist for spherical drops. They also showed that in the case of a spherical bubble, the Basset term disappears, leaving only the new memory term. They thus concluded that the Basset term is a very special form of the memory terms, which only occurs for no-slip spheres. Therefore, if either the spherical shape or the no-slip boundary condition is relaxed, an additional memory term can occur with its behaviour qualitatively different from the Basset term, as also mentioned by Yang & Leal (1991).

Along the lines suggested by Yang & Leal (1991), Magnaudet & Legendre (1998) extended the fixed radius analysis to a spherical bubble whose radius can vary with time, showing that a history force can also result from bubble radius variation. They further identified that the history force can be unimportant if the Reynolds number based on the bubble translational speed or that based on the radial velocity due to bubble shrinking is smaller than unity. Takemura & Magnaudet (2004) experimentally examined the rising motion of a shrinking bubble. They found that the force expression based on the zero-Reynolds-number analysis actually overpredicts the history force due to finite-Reynolds-number effects. In the experimental work by Garbin *et al.* (2009), ultrasound was used to make microbubbles translate unsteadily and a time-resolved study of their motion was performed. The hydrodynamic forces

extracted from the data indicated that the history force actually contributes the most part of the drag force and thus is crucial to giving a correct account of the unsteady motion of microbubbles.

It is worth mentioning that in practice a bubble might inevitably be contaminated by impurities or surfactants on its surface. In this case, the bubble will no longer be shear-free as normally assumed and thus allow partial slip on its surface, acting between no-slip and perfect-slip situations. The situation is somewhat similar to that of the study by Michaelides & Feng (1995) who included interfacial slip in the unsteady motion of a drop in another viscous fluid. They showed that the additional interfacial slip can significantly modify the history terms compared to those without slip.

As such, it might appear that the asphericity and fluidity of a particle are not the sole causes responsible for an additional memory term. Even for a rigid spherical particle, a distinct memory term can also arise from the existence of fluid slippage on the particle surface (Albano *et al.* 1975; Michaelides & Feng 1995; Gatignol 2007). And yet, these previous studies merely derived the force laws but were not aware of non-trivial effects brought about by slip. Specifically, they did not recognize that the extent of slip actually changes with frequency or time. In the high-frequency or short-time regime, in particular, the extent of slip could become so large that it can completely change the nature of the memory term. The purpose of this article is to fill this gap.

When there exists a surface slip in an unsteady fluid motion, what might be missing in the physics lies in the fact that the extent of slip is not determined by the slip length λ alone, but by its size relative to the boundary layer thickness δ that constantly changes with time. As will be shown, this competition between λ and δ will completely change the nature of the memory term, which is very different from those for non-spherical or fluid particles (Lawrence & Weinbaum 1986; Yang & Leal 1991; Galindo & Gerbeth 1993). We also find that no matter how small λ is, its impacts will always persist at sufficiently high frequencies for an oscillatory particle motion. This will in turn change the frequency responses of the amplitude and phase of the history force. Similar characteristic changes can also occur to the short-term force response in a transient particle motion.

To see how slip modifies the unsteady force response, we begin with the force on a no-slip sphere that undergoes an oscillatory motion $U = U_0 \mathrm{e}^{-\mathrm{i}\omega t}$ at frequency ω in a fluid of viscosity μ (Lawrence & Weinbaum 1986):

$$F = -6\pi\mu U_0 a \left(1 + \sqrt{2}\mathrm{e}^{-\mathrm{i}(\pi/4)}\frac{1}{\hat{\delta}} + \frac{2}{9}\mathrm{e}^{-\mathrm{i}(\pi/2)}\frac{1}{\hat{\delta}^2}\right)\mathrm{e}^{-\mathrm{i}\omega t}. \tag{1.1}$$

Here U_0 is the peak velocity and $\hat{\delta}(\omega) = \delta(\omega)/a$ is the Stokes boundary layer thickness $\delta(\omega) = (2\nu/\omega)^{1/2}$ normalized by the sphere's radius a, where ν is the kinematic viscosity of the fluid. The first, second and third terms on the right-hand side of (1.1) represent the Stokes drag, the Basset force of $O(\hat{\delta}^{-1})$ and the added mass of $O(\hat{\delta}^{-2})$, respectively. Note also that the latter two have phases $\pi/4$ and $\pi/2$ ahead of the first.

As can be clearly revealed in (1.1), the Basset history term, which scales as $\mu U_0 a^2/\delta$, is essentially the result of the viscous stress $\tau_s \sim \mu U_0/\delta$ across the boundary layer thickness δ. It is also this term contributing to the $t^{-1/2}$ kernel function in the memory integral if the particle translates in an arbitrary time-dependent manner. When there is slip on the particle surface, however, because not all the momentum from the particle can be transmitted into the fluid, the fluid on the surface will slide at a speed

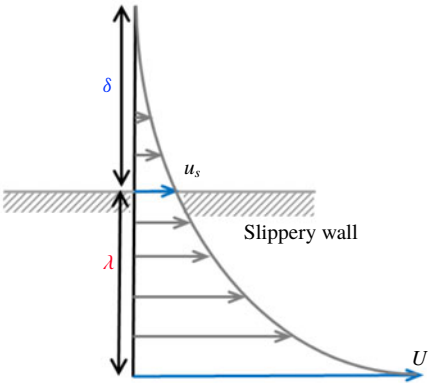

FIGURE 1. (Colour online) Illustration of the dynamic slip effect with the fluid velocity profile driven by an oscillating slippery plate. The extent of slip here is not fixed but constantly changes with the time-varying Stokes boundary layer thickness δ relative to the slip length λ. At a sufficiently high frequency where δ is much thinner than λ, the surface velocity u_s will be $O(\delta/\lambda)$ slower than the plate speed U, leading to a constant wall stress $\mu U/\lambda$.

slower than that of the particle. The situation is similar to that of fluid motion driven by an oscillating slippery plate (Fujioka & Wei 2018). As illustrated in figure 1, because the fluid velocity at the surface now is slowed down to $u_s \sim U\delta/(\lambda+\delta)$, the corresponding viscous stress is reduced to $\tau_s \sim \mu u_s/\delta \sim \mu U/(\lambda+\delta)$. But if the oscillation frequency ω is so high that $\delta \sim (\nu/\omega)^{1/2}$ is much thinner than λ, τ_s will become a constant $\sim\mu U/\lambda$. This completely changes the characteristics of the history force in that not only will the force become $\mu U a^2/\lambda$, independent of ω, but also it will be *in phase* with the driving velocity U. With the above picture in mind, below we revisit the Basset problem with surface slip to give a more in-depth account of how the history force changes its characteristics due to slip effects.

2. Oscillatory translation of a slippery sphere

Consider the oscillatory motion of a slippery spherical particle of radius a moving with velocity $\boldsymbol{U} = U(t)\boldsymbol{e}_z = U_0\exp(-\mathrm{i}\omega t)\boldsymbol{e}_z$ in a viscous fluid of density ρ and viscosity μ. If the Reynolds number $Re = \rho U_0 a/\mu$ is sufficiently small, the fluid motion around the particle can be approximately described by the unsteady linearized Navier–Stokes equation:

$$\rho\left[\frac{\partial \boldsymbol{v}}{\partial t}\right] = -\nabla p + \mu\nabla^2\boldsymbol{v}. \tag{2.1}$$

Here $\boldsymbol{v} = v_r\boldsymbol{e_r} + v_\theta\boldsymbol{e_\theta}$ is the velocity field with v_r and v_θ being the velocity components in the r and θ directions, respectively. Also, p is the pressure and t is time. We write the flow field in terms of stream function ψ such that $v_r = (1/r^2\sin\theta)(\partial\psi/\partial\theta)$ and $v_\theta = -(1/r\sin\theta)(\partial\psi/\partial r)$ satisfy the continuity equation $\nabla\cdot\boldsymbol{v} = 0$. Equation (2.1) is reduced to

$$\left(E^2 - \frac{1}{\nu}\frac{\partial}{\partial t}\right)E^2\psi = 0, \tag{2.2}$$

with $E^2 = \partial^2/\partial r^2 + \sin\theta/r^2(\partial/\partial\theta)(1/\sin\theta(\partial/\partial\theta))$. Similar to Basset (1888), the solution to (2.2) takes the following form (Landau & Lifshitz 1987; Yih 1977):

$$\psi = \sin^2\theta f(r)\mathrm{e}^{-\mathrm{i}\omega t}, \tag{2.3}$$

$$f = \frac{A}{r} + B\left(\frac{1}{r} - \mathrm{i}k\right)\mathrm{e}^{\mathrm{i}kr}, \tag{2.4}$$

where $k = (1+\mathrm{i})/\delta$ and $\delta = (2\nu/\omega)^{1/2}$. With the Navier slip condition $(\boldsymbol{v}-\boldsymbol{U})\cdot(\boldsymbol{I}-\boldsymbol{nn}) = \lambda(\nabla\boldsymbol{v}+(\nabla\boldsymbol{v})^{\mathrm{T}})\cdot\boldsymbol{n}\cdot(\boldsymbol{I}-\boldsymbol{nn})$ and the impenetrable condition $(\boldsymbol{v}-\boldsymbol{U})\cdot\boldsymbol{n} = 0$ on the particle surface $r = a$ (with $\boldsymbol{n}$ being the surface normal vector):

$$v_\theta + U\sin\theta = \lambda\left[r\frac{\partial}{\partial r}\left(\frac{v_\theta}{r}\right) + \frac{1}{r}\frac{\partial v_r}{\partial\theta}\right], \tag{2.5}$$

$$v_r = U\cos\theta, \tag{2.6}$$

the constants A and B in (2.4) can be determined as

$$\frac{A}{a^3} = \frac{1}{2} - \frac{3}{2}\left(\frac{1+2\dfrac{\lambda}{a}}{1+(3-\mathrm{i}ka)\dfrac{\lambda}{a}}\right)\frac{(1-\mathrm{i}ka)}{a^2k^2}, \tag{2.7}$$

$$\frac{B}{a^3} = \frac{3}{2}\left(\frac{1+2\dfrac{\lambda}{a}}{1+(3-\mathrm{i}ka)\dfrac{\lambda}{a}}\right)\frac{\mathrm{e}^{-\mathrm{i}ka}}{a^2k^2}. \tag{2.8}$$

Having determined the flow field from (2.3), the pressure can be evaluated as $p = -\mu U_0\cos\theta Ak^2/r^2$ after substituting the flow field into (2.1). The hydrodynamic force on the particle in the direction of its movement can be evaluated using

$$F = 2\pi a^2\int_0^\pi(\tau_{rr}\cos\theta - \tau_{r\theta}\sin\theta)_{r=a}\sin\theta\,\mathrm{d}\theta. \tag{2.9}$$

With the normal stress $\tau_{rr} = -p + 2\mu(\partial v_r/\partial r)$ and the tangential stress $\tau_{r\theta} = \mu[r(\partial/\partial r)(v_\theta/r) + (1/r)(\partial v_r/\partial\theta)]$, equation (2.9) yields $F = F(\omega)\mathrm{e}^{-\mathrm{i}\omega t}$ with

$$F(\omega) = -6\pi\mu U_0 a\left[\left(\frac{1+2\hat{\lambda}}{1+3\hat{\lambda}}\right)\left(\frac{1+\sqrt{2}\mathrm{e}^{-\mathrm{i}(\pi/4)}\dfrac{1}{\hat{\delta}}}{1+\dfrac{\hat{\lambda}}{1+3\hat{\lambda}}\sqrt{2}\mathrm{e}^{-\mathrm{i}(\pi/4)}\dfrac{1}{\hat{\delta}}}\right) + \frac{2}{9}\mathrm{e}^{-\mathrm{i}(\pi/2)}\frac{1}{\hat{\delta}^2}\right], \tag{2.10}$$

where $\hat{\lambda} = \lambda/a$ and $\hat{\delta}(\omega) = \delta/a = (2\nu/\omega a^2)^{1/2}$ are the dimensionless slip length and boundary layer thickness, respectively. Note that the force expression here is obtained by evaluating (2.9) while keeping the sphere fixed. Since the inertial term $\rho\boldsymbol{v}\cdot\nabla\boldsymbol{v}$ in (2.1) is assumed negligible because of small Re, even though the particle undergoes an oscillatory translation, the fluid motion around it is essentially described in an inertial reference frame and the corresponding force is thus Galileo invariant. We also remark that although the same result was obtained previously (Albano *et al.* 1975; Michaelides & Feng 1995), those studies did not recognize non-trivial force

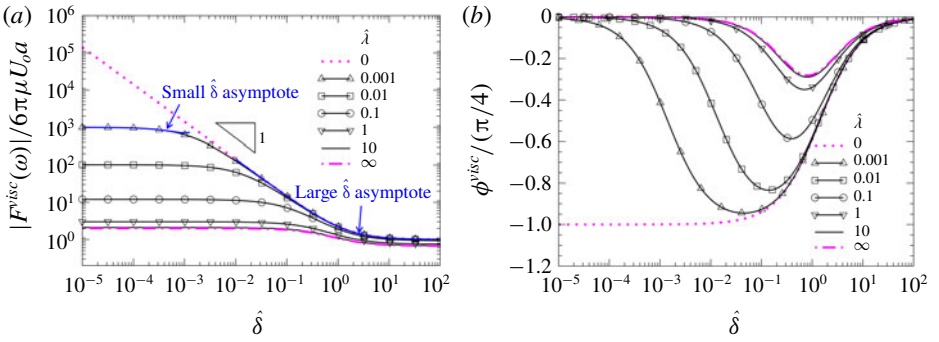

FIGURE 2. (Colour online) (*a*) Plot of the force amplitude $|F^{visc}(\omega)|/6\pi\mu U_0 a$ against $\hat{\delta}$ for different values of dimensionless slip length $\hat{\lambda}$. In the small $\hat{\delta}$ regime, the no-slip $\hat{\lambda}=0$ case shows the Basset $1/\hat{\delta}$ decay. In contrast, for the slip case, a plateau at the level $\sim\hat{\lambda}^{-1}$ and its persistence until the SST point $\hat{\delta}\sim\hat{\lambda}^{-1}$ can be observed. Both small and large $\hat{\delta}$ asymptotes are drawn for $\hat{\lambda}=0.001$. (*b*) Plot of the corresponding phase ϕ^{visc} as a function of $\hat{\delta}$, showing that ϕ^{visc} will jump from the no-slip value $-\pi/4$ to zero as $\hat{\delta}\to 0$ regardless of any non-zero value of $\hat{\lambda}$.

responses due to surface slip, especially for how the viscous part varies with $\hat{\delta}$, which is demonstrated below.

It is easy to see from (2.10) that $\hat{\lambda}=0$ recovers the no-slip result (1.1). Let F^{visc} represent the viscous part of (2.10):

$$F^{visc}=-6\pi\mu U_0 a\left(\frac{1+2\hat{\lambda}}{1+3\hat{\lambda}}\right)\left(\frac{1+\sqrt{2}\mathrm{e}^{-\mathrm{i}(\pi/4)}\dfrac{1}{\hat{\delta}}}{1+\dfrac{\hat{\lambda}}{1+3\hat{\lambda}}\sqrt{2}\mathrm{e}^{-\mathrm{i}(\pi/4)}\dfrac{1}{\hat{\delta}}}\right). \tag{2.11}$$

Compared to (1.1), slip modifies F^{visc} in two ways. First, the steady drag is reduced by a factor of $(1+2\hat{\lambda})/(1+3\hat{\lambda})$. It is essentially identical to the Hadamard–Rybczynski formula for the steady drag on a spherical liquid drop in that $\hat{\lambda}$ here can be analogous to the viscosity ratio of the bulk fluid to the drop. This drag in the no-slip $\hat{\lambda}\to 0$ limit recovers the Stokes drag $6\pi\mu U_0 a$. In the perfect-slip $\hat{\lambda}\to\infty$ limit where the particle surface becomes shear-free, the drag is reduced to $4\pi\mu U_0 a$, coinciding with that on a bubble. Second, the frequency-dependent $1/\hat{\delta}$ parts further involve an additional contribution $(1+3\lambda)^{-1}\times\sqrt{2}\mathrm{e}^{-\mathrm{i}\pi/4}\hat{\lambda}/\hat{\delta}$ that can compete with the Basset term $\sqrt{2}\mathrm{e}^{-\mathrm{i}\pi/4}/\hat{\delta}$. These modifications due to slip will not only change the amplitude of $F^{visc}(\omega)$ but also influence its phase behaviour when varying $\hat{\delta}(\omega)$ with ω.

Figure 2(*a*) plots the force amplitude $|F^{visc}(\omega)|/6\pi\mu U_0 a$ against $\hat{\delta}$ for various values of $\hat{\lambda}$. For the no-slip $\hat{\lambda}=0$ case, it shows a typical Basset $1/\hat{\delta}$ decay in the small $\hat{\delta}$ regime at high ω and a steady asymptote in the large $\hat{\delta}$ regime at low ω. When there is surface slip, the force decreases with $\hat{\delta}$ in a similar manner. But in the small $\hat{\delta}$ regime, instead of the Basset $1/\hat{\delta}$ decay, we find a plateau for $\hat{\delta}$ below some critical value. In particular, no matter how small $\hat{\lambda}$ is, it can always turn the $1/\hat{\delta}$ decay into a

plateau – the larger the value of $\hat{\lambda}$, the wider the range of $\hat{\delta}$ within which the plateau is sustained. In this case, the plateau is found to be $\sim\hat{\lambda}^{-1}$ and persists until increasing $\hat{\delta}$ to the turning point at $\hat{\delta}\sim\hat{\lambda}$ or $\omega\sim\nu/\lambda^2$. The latter also marks the slip–stick transition (SST) point where the force starts to follow the usual Basset $1/\hat{\delta}$ decay.

Such change in the force response due to slip becomes even more evident when plotting the corresponding phase $\phi^{visc}=\tan^{-1}[\mathrm{Im}(F^{visc}(\omega))/\mathrm{Re}(F^{visc}(\omega))]$ as a function of $\hat{\delta}$, as shown in figure 2(*b*). In the case of no slip, ϕ^{visc} starts from the $\hat{\delta}\to 0$ asymptote $-\pi/4$ and then monotonically increases with $\hat{\delta}$ towards zero in the $\hat{\delta}\to\infty$ limit. In contrast, when there is slip on the particle surface, the behaviour of ϕ^{visc} is not monotonic – it exhibits an inverted bell in a range of $\hat{\delta}$. In particular, ϕ^{visc} will jump from $-\pi/4$ to zero as $\hat{\delta}\to 0$ regardless of the amount of slip.

To better elucidate the features seen in figure 2, we carry out a small $\hat{\delta}$ expansion of (2.11) for $F^{visc}(\omega)$:

$$\frac{F^{visc}(\omega)}{-6\pi\mu U_0 a}=\left(\frac{1+2\hat{\lambda}}{\hat{\lambda}}\right)\left(1-\left(\frac{1+2\hat{\lambda}}{\hat{\lambda}}\right)\frac{\mathrm{e}^{\mathrm{i}(\pi/4)}}{\sqrt{2}}\hat{\delta}\right)+O(\hat{\delta}^2). \tag{2.12}$$

At leading order, $(1+2\hat{\lambda})/\hat{\lambda}$ gives exactly the plateau value with zero phase shift. For small $\hat{\lambda}$, the plateau value reduces to $\hat{\lambda}^{-1}$, exactly corresponding to the constant viscous stress $\tau_s\sim\mu U/\lambda$ when $\delta\ll\lambda$, as in figure 1. At $O(\hat{\delta})$, it not only decreases the force from the plateau value but also causes a phase shift. More importantly, the plateau with small $\hat{\lambda}$ will start to decline at around the SST point $\hat{\delta}\sim\hat{\lambda}$. In contrast, for large $\hat{\lambda}$ under which the particle acts like a bubble, the plateau force is merely twice the Stokes drag with the transition point $\hat{\delta}\sim O(1)$. These results also agree with those for the bubble case obtained by Yang & Leal (1991).

To capture the $1/\hat{\delta}$ decay after the SST point, it is necessary to inspect the behaviour of $F^{visc}(\omega)$ at large $\hat{\delta}$. Taking a small $1/\hat{\delta}$ expansion for (2.11), we get

$$\frac{F^{visc}(\omega)}{-6\pi\mu U_0 a}=\left(\frac{1+2\hat{\lambda}}{1+3\hat{\lambda}}\right)\left(1+\left(\frac{1+2\hat{\lambda}}{1+3\hat{\lambda}}\right)\frac{\sqrt{2}\mathrm{e}^{-\mathrm{i}(\pi/4)}}{\hat{\delta}}\right)+O(\hat{\delta}^{-2}). \tag{2.13}$$

As $\hat{\delta}\to\infty$ the steady drag $F^{visc}(\omega)=-6\pi\mu U_0 a(1+2\hat{\lambda})/(1+3\hat{\lambda})$ is recovered. The $O(\hat{\delta}^{-1})$ term represents the Basset term modified by slip, tending to increase $F^{visc}(\omega)$ as $\hat{\delta}$ is decreased. In addition, the Basset $1/\hat{\delta}$ signature will become more apparent when decreasing $\hat{\delta}$ to $O(1)$ or smaller, as also shown in figure 2(*a*).

As for the phase ϕ^{visc}, its behaviour can be revealed from its tangent value $[\mathrm{Im}(F^{visc}(\omega))/\mathrm{Re}(F^{visc}(\omega))]$ determined from (2.11):

$$\tan(\phi^{visc})=\frac{\hat{\delta}(\beta-1)}{(1+\hat{\delta})(\beta+\hat{\delta})+\beta}, \tag{2.14}$$

where $\beta=\hat{\lambda}/(1+3\hat{\lambda})$. For $\hat{\lambda}=0$, equation (2.14) reduces to $\tan(\phi^{visc})=-1/(1+\hat{\delta})$ which gives the Basset phase $-\pi/4$ as $\hat{\delta}\to 0$. For $\hat{\lambda}\neq 0$, a small $\hat{\delta}$ expansion of (2.14) gives

$$\tan(\phi^{visc})=-\left(1+\frac{1}{2\hat{\lambda}}\right)\hat{\delta}+O(\hat{\delta}^2). \tag{2.15}$$

As a result, as long as slip exists on the particle surface, it will make $\phi^{visc}(\hat{\delta} \to 0)$ jump from the no-slip value $-\pi/4$ to zero, regardless of the amount of slip. Because $\phi^{visc}(\hat{\delta} \to \infty) = 0$, such a phase jump as $\hat{\delta} \to 0$ due to slip implies a maximum phase shift $(\phi^{visc})^*$ at $\hat{\delta} = \hat{\delta}^*$, as seen in figure 2(*b*). Using (2.14), this maximum phase shift is located at

$$\hat{\delta}^* = \sqrt{2}\beta^{1/2}, \tag{2.16}$$

$$(\phi^{visc})^* = \tan^{-1}\left(\frac{\beta - 1}{1 + 2\sqrt{2}\beta^{1/2} + \beta}\right). \tag{2.17}$$

For small $\hat{\lambda}$, the above reduce to $\hat{\delta}^* \approx \sqrt{2}\hat{\lambda}^{1/2}$ and $(\phi^{visc})^* \approx -\pi/4 + \sqrt{2}\hat{\lambda}^{1/2}$. Compared to $\hat{\delta}^* = 0$ and $(\phi^{visc})^* = -\pi/4$ for the no-slip case, the corrections due to slip are $\sqrt{2}\hat{\lambda}^{1/2}$. So the effects of slip on the maximum phase shift are not of $O(\hat{\lambda})$, but amplified to $O(\hat{\lambda}^{1/2})$, which is another feature sensitive to the amount of slip. Note that because $\beta \to 1/3$ as $\hat{\lambda} \to \infty$, the maximum phase shift will never fall below $(\phi^{visc})^* = \tan^{-1}(-(2+\sqrt{6})^{-1}) \approx -0.221$ at $\delta^* = (2/3)^{1/2} \approx 0.816$ in the bubble $\hat{\lambda} \to \infty$ limit, as also shown in figure 2(*b*).

If the particle is moving in an arbitrary time-dependent manner, the force law can be obtained in the same fashion by expressing the particle velocity as a Fourier integral $U(t) = (2\pi)^{-1}\int_{-\infty}^{\infty} U(\omega)\mathrm{e}^{-\mathrm{i}\omega t}\,\mathrm{d}\omega$ with $U(\omega) = \int_{-\infty}^{\infty} U(t)\mathrm{e}^{\mathrm{i}\omega t}\,\mathrm{d}t$. Converting the Fourier transform to a Laplace transform with $-\mathrm{i}\omega \to s$, we can rewrite (2.10) in terms of the Laplace variable s:

$$\frac{F(s)}{-6\pi\mu a} = \left(\left(\frac{1+2\hat{\lambda}}{1+3\hat{\lambda}}\right)\left(\frac{1+t_\nu^{1/2}s^{1/2}}{1+\beta t_\nu^{1/2}s^{1/2}}\right)\left(\frac{1}{s}\right) + \frac{t_\nu}{9}\right) sU(s), \tag{2.18}$$

where $t_\nu = a^2/\nu$ is the viscous diffusion time and $\beta = \hat{\lambda}/(1+3\hat{\lambda})$. Assume that the particle starts from $U = 0$ for $t < 0$ and moves at $U = U(t)$ for $t \geqslant 0$. Following the procedures given in appendix A, we take an inverse Laplace transform and apply the convolution theorem for (2.18). The drag force on the particle is found to be

$$\frac{F(t)}{-6\pi\mu a} = \left(\frac{1+2\hat{\lambda}}{1+3\hat{\lambda}}\right)U + \frac{(1+2\hat{\lambda})^2}{\hat{\lambda}(1+3\hat{\lambda})}\int_0^t \frac{\mathrm{d}U}{\mathrm{d}t'}G(t-t')\,\mathrm{d}t' + \frac{1}{9}t_\nu\frac{\mathrm{d}U}{\mathrm{d}t}, \tag{2.19}$$

where the memory kernel is

$$G(t) = \exp(\beta^{-2}t/t_\nu)\mathrm{erfc}\left(\beta^{-1}\sqrt{t/t_\nu}\right). \tag{2.20}$$

Equation (2.19) agrees with the result obtained previously (Gatignol 2007; Michaelides & Feng 1995). In the no-slip $\hat{\lambda} \to 0$ limit, $G(t) \to (\hat{\lambda}/\sqrt{\pi})\sqrt{t_\nu/t}$ reduces the memory integral to the Basset integral. Equation (2.19) also recovers the result in the bubble $\hat{\lambda} \to \infty$ limit obtained by Yang & Leal (1991).

If $U(t) = U_0$ (const.) for $t \geqslant 0$, the particle will experience a force

$$\frac{F(t)}{-6\pi\mu a} = \left(\frac{1+2\hat{\lambda}}{1+3\hat{\lambda}}\right)U_0 + \frac{(1+2\hat{\lambda})^2}{\hat{\lambda}(1+3\hat{\lambda})}G(t)U_0 + \frac{1}{9}t_\nu U_0\delta(t). \tag{2.21}$$

For short time $t/t_\nu \ll 1$, $G(t) = 1 - (2/\sqrt{\pi})\beta^{-1}(t/t_\nu)^{1/2} + O(t/t_\nu)$. The viscous part in (2.21) is reduced to

$$\frac{F^{visc}(t)}{-6\pi\mu a} \approx \left(\frac{1+2\hat{\lambda}}{\hat{\lambda}}\right)\left(1 - \frac{2}{\sqrt{\pi}}\left(\frac{1+2\hat{\lambda}}{\hat{\lambda}}\right)\left(\frac{t}{t_\nu}\right)^{1/2}\right) U_0, \tag{2.22}$$

which exactly corresponds to (2.12). Note that the factor $\hat{\lambda}^{-1}$ here comes from the memory term G – it is exactly this factor responsible for the plateau due to a thin boundary layer. Now consider the case of small $\hat{\lambda}$. As $t \to 0$, equation (2.22) reveals that the particle will experience a constant drag force $6\pi\mu a U_0/\hat{\lambda}$ due to the constant stress $\mu U_0/\lambda$ on the particle surface. This force will start to exhibit a $t^{1/2}$ decrease at a time around the SST point $t \sim \hat{\lambda}^2 t_\nu = \lambda^2/\nu$ when the boundary layer thickness $\delta \sim (\nu t)^{1/2}$ grows to a size of about λ. We emphasize that while a similar constant force $12\pi\mu a U_0$ followed by a $t^{1/2}$ decrease can still occur to the bubble limit as $\lambda \to \infty$, the time scale to see a transition from the former to the latter is always at around the characteristic viscous time a^2/ν. So such constant force and SST point, which respond solely to λ, will be the exclusive features when surface slip is present.

Finally, we should emphasize that for unsteady Stokes motion, generally there is no one-to-one correspondence between an arbitrary slip length of a slippery solid particle and an arbitrary viscosity ratio of the drop to the outer fluid (except for the $\hat{\lambda} \to \infty$ limit). For the drop case, it has been shown by Yang & Leal (1991) and Galindo & Gerbeth (1993) that while the additional memory kernel is finite as $t \to 0$, the whole memory kernel is still dominated by the $t^{-1/2}$ Basset kernel that diverges as $t \to 0$, regardless of the viscosity ratio (except for the bubble limit under which the Basset term vanishes). For the slip case, on the other hand, the memory kernel is always finite as $t \to 0$. This difference is mainly attributed to different surface boundary conditions between these two cases. For a viscous drop, the fluid velocities inside and outside the drop have to be matched on the drop surface. For this reason, a sudden movement of the drop will cause developments of boundary layers of $\delta \propto t^{1/2}$ along both sides of the drop surface. Because the corresponding shear stresses vary as $1/\delta \propto t^{-1/2}$ and are also continuous at the drop surface, this leads to a divergence in the force on the drop as $t \to 0$. This $t^{-1/2}$ Basset force will start to relax when δ grows to a size of about the particle radius a, giving the transition time $\sim a^2/\nu$.

In contrast, for a slippery solid particle, because of the slip condition (2.5), there is always a jump between the particle velocity and the fluid velocity on the particle surface. At a sufficiently short time where the boundary layer is thin and $\delta \ll \lambda$, such a velocity jump will be nearly equal to the particle velocity, saturated with a constant shear stress $\sim \mu U/\lambda$ due to strong slip effects. This gives rise to the constant force plateau in (2.22) or the saturation of the history force seen in figure 2(*a*). The constant force plateau will persist until δ grows to a size of about the slip length λ, giving the SST time $\sim \lambda^2/\nu$.

3. Rotary oscillation of a slippery sphere

We also examine the oscillatory rotation of a slippery sphere with angular velocity $\Omega(t) = \Omega_0 e^{-i\omega t}$. Following Ashmawy (2012), the azimuthal fluid velocity is governed by $(E^2 - \nu^{-1}\partial/\partial t)[r \sin\theta v_\phi(r, \theta, t)] = 0$ with the solution $v_\phi = cf(r)\sin\theta e^{-i\omega t}$, where $f(r) = (1/r + 1/(k_1 r^2))e^{-k_1(r-a)}$ with $k_1 = (-i\omega/\nu)^{1/2}$. Applying the slip boundary condition on the surface of the sphere at $r = a$:

$$\{v_\phi(a, \theta, t) - \Omega(t) a \sin\theta\} = \lambda \tau_{r\phi}/\mu, \tag{3.1}$$

with $\tau_{r\phi} = \mu r(\partial/\partial r)(v_\phi/r)_{r=a}$ being the azimuthal stress evaluated at the surface, the coefficient c can be determined as $c = \Omega_0 k_1 a^3/(\hat{\lambda}k_1^2a^2 + (k_1a+1)(1+3\hat{\lambda}))$. The torque acting on the sphere can then be determined as $T_z = 2\pi a^3 \int_0^\pi \tau_{r\phi}|_{r=a} \sin^2\theta \, \mathrm{d}\theta = T_z(\omega)\mathrm{e}^{-\mathrm{i}\omega t}$ with $T_z(\omega)$ given by

$$\frac{T_z(\omega)}{-8\pi\mu\Omega_0 a^3} = \frac{1+\sqrt{2}\mathrm{e}^{-\mathrm{i}(\pi/4)}\dfrac{1}{\hat{\delta}}+\dfrac{2}{3}\mathrm{e}^{-\mathrm{i}(\pi/2)}\dfrac{1}{\hat{\delta}^2}}{1+\sqrt{2}\mathrm{e}^{-\mathrm{i}(\pi/4)}\dfrac{1}{\hat{\delta}}+3\hat{\lambda}\left[1+\sqrt{2}\mathrm{e}^{-\mathrm{i}(\pi/4)}\dfrac{1}{\hat{\delta}}+\dfrac{2}{3}\mathrm{e}^{-\mathrm{i}(\pi/2)}\dfrac{1}{\hat{\delta}^2}\right]}. \tag{3.2}$$

So slip modifies not only the steady torque, but also both the $\hat{\delta}^{-1}$ and $\hat{\delta}^{-2}$ parts. This is different from the translational case in which only the $\hat{\delta}^{-2}$ added mass term remains unchanged in the force response (2.10). Why the added mass can vary with slip in the rotational case but not in the translational case can be understood as follows. For the translational case, the added mass actually comes from potential dipole that dominates at high frequencies. Because the dipole field is irrotational, the corresponding force is independent of viscosity and hence of the amount of slip.

In contrast, when the particle undergoes rotary oscillations, it is force-free as it can be thought of as a couple of two oppositely acting forces on the particle. Because this force couple can only be implemented through the viscous shearing over the particle surface – the pressure $p = 0$ everywhere – the partial fluid displacement by this oscillating force couple, which gives the added mass, is also carried out by such shearing. Since the larger the slip the weaker the shearing, the resulting added mass will be attenuated with the amount of slip. For the same reason, both the steady $\hat{\delta}^0$ and the Basset $\hat{\delta}^{-1}$ contributions will also be reduced by slip in the same manner. So for large $\hat{\lambda}$, the torque (3.2) is reduced to $T_z(\omega) \approx -8\pi\mu\Omega_0 a^3/3\hat{\lambda}$. In the bubble limit as $\hat{\lambda} \to \infty$, $T_z(\omega) \to 0$ since no viscous shear can be generated on the particle surface.

Figure 3(*a*) plots the torque amplitude $|T_z(\omega)|/8\pi\mu\Omega_0 a^3$ against $\hat{\delta}$ for different values of $\hat{\lambda}$. For the no-slip $\hat{\lambda} = 0$ case, the torque first displays the Basset $\hat{\delta}^{-1}$ decay for $\hat{\delta} < 1$ and then turns towards a constant for $\hat{\delta} > 1$, in accordance with the small $\hat{\delta}$ expansion of (3.2) with $\hat{\lambda} = 0$:

$$\frac{T_z(\omega)}{-8\pi\mu\Omega_0 a^3} = \frac{2}{3}\left[\frac{\mathrm{e}^{-\mathrm{i}(\pi/4)}}{\sqrt{2}}\frac{1}{\hat{\delta}}+1\right] + O(\hat{\delta}). \tag{3.3}$$

In contrast, when there is slip, especially with small $\hat{\lambda}$ such as 10^{-3}–10^{-1}, we again find an apparent plateau at the level $\sim(3\hat{\lambda})^{-1}$ followed by $1/\hat{\delta}$ decay for $\hat{\delta}$ beyond the SST point $\hat{\delta} \sim \hat{\lambda}$. The above features are in agreement with the small $\hat{\delta}$ expansion of (3.2):

$$\frac{T_z(\omega)}{-8\pi\mu\Omega_0 a^3} = \frac{1}{3\hat{\lambda}}\left[1 - \frac{1}{\sqrt{2}}\mathrm{e}^{\mathrm{i}(\pi/4)}\frac{\hat{\delta}}{\hat{\lambda}}\right] + O(\hat{\delta}^2), \tag{3.4}$$

which is rather different from (3.3) for $\hat{\lambda} = 0$. Note here that the leading term $(3\hat{\lambda})^{-1}$ comes from the added mass $\hat{\delta}^{-2}$ term. This also coincides with the leading contribution to the torque for $\hat{\lambda} \gg 1$. As also indicated by (3.4), slip can introduce a phase jump at $\hat{\delta} = 0$ with respect to the no-slip case and hence give rise to a non-monotonic phase change with varying $\hat{\delta}$, as displayed in figure 3(*b*).

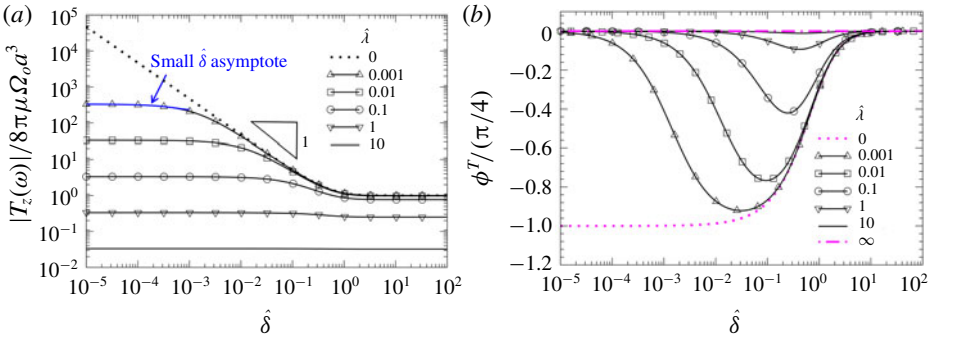

FIGURE 3. (Colour online) (*a*) Plot of the torque amplitude $|T_z(\omega)|/8\pi\mu\Omega_0 a^3$ against $\hat{\delta}$ for different values of $\hat{\lambda}$. For small $\hat{\lambda}$, an apparent plateau at the level $\sim(3\hat{\lambda})^{-1}$ followed by $1/\hat{\delta}$ decay for $\hat{\delta}$ beyond the SST point $\hat{\delta}\sim\hat{\lambda}$ can be observed, similar to those shown in figure 2(*a*) for the force response in the translational case. The small $\hat{\delta}$ asymptote is drawn for $\hat{\lambda}=0.001$. (*b*) Plot of the corresponding phase ϕ^{T} against $\hat{\delta}$, showing that slip can cause a phase jump as $\hat{\delta}\to 0$ with respect to the $\hat{\lambda}=0$ case and a non-monotonic phase change with varying $\hat{\delta}$, similar to figure 2(*b*).

How the phase ϕ^T varies with $\hat{\delta}$ and $\hat{\lambda}$ can be revealed from its tangent value $[\mathrm{Im}(T_z(\omega))/\mathrm{Re}(T_z(\omega))]$ determined from (3.2):

$$\tan(\phi^{\mathrm{T}})=-\frac{2}{3}\left(\frac{1}{1+3\hat{\lambda}}\right)\frac{\hat{\delta}^{-2}}{1+(1+\hat{\delta}^{-1})^{-1}\left(\hat{\delta}^{-1}+\dfrac{2}{3}\hat{\delta}^{-2}\right)\left(\hat{\delta}^{-1}+\hat{\delta}^{-2}\dfrac{2\hat{\lambda}}{1+3\hat{\lambda}}\right)}. \tag{3.5}$$

For $\hat{\lambda}=0$, expanding (3.5) in a small $\hat{\delta}$ yields $\tan(\phi^{\mathrm{T}})\approx-1+\hat{\delta}/2$, which gives the Basset phase $\phi^{\mathrm{T}}=-\pi/4$ as $\hat{\delta}\to 0$. In contrast, when $\hat{\lambda}\neq 0$, a small $\hat{\delta}$ expansion of (3.5) results in $\tan(\phi^{\mathrm{T}})\approx-\hat{\delta}/2\hat{\lambda}$, making $\phi^{\mathrm{T}}(\hat{\delta}\to 0)$ jump from the no-slip value $-\pi/4$ to zero, regardless of the value of $\hat{\lambda}$ as long as $\hat{\lambda}$ is non-zero. Also, because $\phi^{\mathrm{T}}(\hat{\delta}\to\infty)=0$, ϕ^{T} must vary non-monotonically with $\hat{\delta}$, implying the existence of a maximum phase shift $(\phi^{\mathrm{T}})^*$ at $\hat{\delta}=\hat{\delta}^*$, as seen in figure 3(*b*). Using (3.5), for small $\hat{\lambda}$ we can determine the location of the maximum phase shift as $\delta^*\approx 2\hat{\lambda}^{1/2}$ and $\tan(\phi^{\mathrm{T}})\approx -1+2\hat{\lambda}^{1/2}$, which contribute to $O(\hat{\lambda}^{1/2})$ corrections to the no-slip results. The above features basically resemble those of the translational case considered in § 2. Note that as $\hat{\lambda}\to\infty$, $\tan(\phi^{\mathrm{T}})\to 0$ and hence $\phi^{\mathrm{T}}\to 0$, which is simply due to the fact that $T_z(\omega)\to 0$ as $\hat{\lambda}\to\infty$ from (3.2). This is different from the translational case in which both the viscous force and the maximum phase shift are finite as $\hat{\lambda}\to\infty$.

For an arbitrary time-dependent spinning motion, we again express the angular velocity as a Fourier integral followed by its conversion to a Laplace transform with $-\mathrm{i}\omega\to s$. This leads (3.2) to

$$\frac{T_z(s)}{-8\pi\mu a^3}=\frac{1}{1+3\hat{\lambda}}\left[\frac{1}{s}+\frac{t_v}{3[(1+3\hat{\lambda})(1+s^{1/2}t_v^{1/2})+st_v\hat{\lambda}]}\right]s\Omega(s). \tag{3.6}$$

The derivation of the inverse Laplace transform of (3.6) is given in appendix B. It turns out that distinct forms can result for $\hat{\lambda}=0$, $0<\hat{\lambda}<1$, $\hat{\lambda}>1$ and $\hat{\lambda}=1$, as shown separately below.

3.1. *Case of* $\hat{\lambda}=0$

In the case of no slip, the inverse Laplace transform of (3.6) is

$$\frac{T_z(t)}{-8\pi\mu a^3}=\left[\Omega(t)+\frac{1}{3}\int_0^t\frac{\mathrm{d}\Omega(t')}{\mathrm{d}t'}K_0(t-t')\,\mathrm{d}t'\right], \tag{3.7}$$

with the memory kernel K_0 according to (B 8):

$$K_0=-\mathrm{erfc}\left(\sqrt{t/t_\nu}\right)\exp(t/t_\nu)+\frac{1}{\sqrt{\pi}}\sqrt{\frac{t_\nu}{t}}. \tag{3.8}$$

If the particle is subjected to an impulsive rotation with a constant Ω_0, equation (3.7) is reduced to

$$\frac{T_z(t)}{-8\pi\mu a^3}=\Omega_0\left[1+\frac{1}{3}K_0(t)\right]. \tag{3.9}$$

For short time $t/t_\nu\ll 1$, $K_0=(1/\sqrt{\pi})\sqrt{t_\nu/t}-1+O(\sqrt{t/t_\nu})$. So (3.9) becomes

$$\frac{T_z(t)}{-8\pi\mu a^3}\approx\frac{2}{3}\left[\frac{1}{2\sqrt{\pi}}\sqrt{\frac{t_\nu}{t}}+1\right]\Omega_0, \tag{3.10}$$

which exactly corresponds to (3.3). Note that the torque given by (3.10) diverges as $t^{-1/2}$ as $t\to 0$ because $K_0(t\to 0)$ in (3.8) diverges in the same manner. Such divergence will disappear when slip is present, as shown below.

3.2. *Case of* $0<\hat{\lambda}<1$

This case describes the sub slip scenario with $\lambda<a$, which may be most relevant to the actual situation. The torque is found to be

$$\frac{T_z(t)}{-8\pi\mu a^3}=\frac{1}{1+3\hat{\lambda}}\left[\Omega(t)+\frac{1}{3\sqrt{1-\hat{\lambda}}}\int_0^t\frac{\mathrm{d}\Omega(t')}{\mathrm{d}t'}K(t-t')\,\mathrm{d}t'\right], \tag{3.11}$$

where the memory kernel K is found to be (B 10):

$$\begin{aligned}K(t)\;=\;&-(x-y)/(2\hat{\lambda})\times\exp((x^2/2\hat{\lambda}^2)((1+\hat{\lambda})-xy)t/t_\nu)\\&\times\mathrm{erfc}\left((x/2\hat{\lambda})\times(x-y)\sqrt{t/t_\nu}\right)+(x+y)/(2\hat{\lambda})\\&\times\exp((x^2/2\hat{\lambda}^2)((1+\hat{\lambda})+xy)t/t_\nu)\\&\times\mathrm{erfc}\left((x/2\hat{\lambda})\times(x+y)\sqrt{t/t_\nu}\right),\end{aligned} \tag{3.12}$$

with $x=\sqrt{1+3\hat{\lambda}}$ and $y=\sqrt{|1-\hat{\lambda}|}$.

If the particle undergoes a sudden spinning with a constant Ω_0, the particle will experience a torque

$$\frac{T_z(t)}{-8\pi\mu a^3} = \frac{\Omega_0}{1+3\hat{\lambda}}\left[1+\frac{1}{3\sqrt{1-\hat{\lambda}}}K(t)\right]. \tag{3.13}$$

For short time $t/t_\nu \ll 1$, equation (3.12) is reduced to

$$K(t) = \frac{\sqrt{1-\hat{\lambda}}}{\hat{\lambda}} - \frac{2(1+3\hat{\lambda})\sqrt{1-\hat{\lambda}}}{\hat{\lambda}^2\sqrt{\pi}}\left(\frac{t}{t_\nu}\right)^{1/2} + O(t/t_\nu). \tag{3.14}$$

So the leading term $\sqrt{1-\hat{\lambda}}/\hat{\lambda}$ is constant varying only with $\hat{\lambda}$ – it is this term that contributes to the plateau. For $\hat{\lambda} \ll 1$, equation (3.13) is dominated by the memory K term and hence is reduced to

$$\frac{T_z(t)}{-8\pi\mu a^3} \approx \frac{1}{3\hat{\lambda}}\left[1-\frac{2}{\hat{\lambda}\sqrt{\pi}}\left(\frac{t}{t_\nu}\right)^{1/2}\right]\Omega_0. \tag{3.15}$$

Equation (3.15) clearly indicates the plateau value $(3\hat{\lambda})^{-1}$ and its decrease at around the SST point $t \sim \hat{\lambda}^2 t_\nu = \lambda^2/\nu$, exactly corresponding to (3.4). Although the time response forms similar to (3.11) have been given previously (Gatignol 2007; Ashmawy 2012), those studies did not recognize the short-time constant plateau from the memory kernel (3.14).

3.3. *Case of* $\hat{\lambda} > 1$

This case is the super slip situation with $\lambda > a$. The resulting torque takes a form similar to (3.11):

$$\frac{T_z(t)}{-8\pi\mu a^3} = \frac{1}{1+3\hat{\lambda}}\left[\Omega(t)+\frac{1}{3\sqrt{\hat{\lambda}-1}}\int_0^t \frac{\mathrm{d}\Omega(t')}{\mathrm{d}t'}K_1(t-t')\,\mathrm{d}t'\right], \tag{3.16}$$

but has a different memory kernel according to (B 13):

$$\begin{aligned} K_1 \;=\; & 2\mathrm{Im}\left[(x+\mathrm{i}y)/(2\hat{\lambda}) \times \exp((x^2/2\hat{\lambda}^2)((1+\hat{\lambda})+\mathrm{i}xy)t/t_\nu)\right. \\ & \left.\times\, \mathrm{erfc}((x/2\hat{\lambda}) \times (x+\mathrm{i}y)\sqrt{t/t_\nu})\right], \end{aligned} \tag{3.17}$$

where Im means the imaginary part.

If the particle starts with an instantaneous rotation at constant Ω_0, it will experience a torque

$$\frac{T_z(t)}{-8\pi\mu a^3} = \frac{\Omega_0}{1+3\hat{\lambda}}\left[1+\frac{1}{3\sqrt{\hat{\lambda}-1}}K_1(t)\right]. \tag{3.18}$$

For short time $t/t_\nu \ll 1$, the memory kernel (3.17) behaves as

$$K_1 = \frac{\sqrt{\hat{\lambda}-1}}{\hat{\lambda}} - \frac{2(1+3\hat{\lambda})\sqrt{\hat{\lambda}-1}}{\hat{\lambda}^2\sqrt{\pi}}\left(\frac{t}{t_\nu}\right)^{1/2} + O(t/t_\nu). \tag{3.19}$$

Again, it is still dominated by a constant plateau $\sqrt{\hat{\lambda}-1}/\hat{\lambda}$ that varies only with $\hat{\lambda}$. As for the torque (3.18), the plateau term from K_1 actually contributes to $1/(3\hat{\lambda})$ in the bracket of (3.18), which is always less than the steady torque part '1' when $\hat{\lambda} > 1$. Consequently, for $\hat{\lambda} \gg 1$, equation (3.18) will be dominated by the steady torque with an $O((t/t_\nu)^{1/2})$ correction from K_1:

$$\frac{T_z(t)}{-8\pi\mu a^3} \approx \frac{1}{3\hat{\lambda}}\left[1 - \frac{2}{\hat{\lambda}\sqrt{\pi}}\left(\frac{t}{t_\nu}\right)^{1/2}\right]\Omega_0. \tag{3.20}$$

Interestingly, equation (3.20) is identical to (3.15) for $\hat{\lambda} \ll 1$ despite the fact that the latter is dominated by the plateau from the memory term. In fact, the short-time torque expression (3.20) is always true for any value of $\hat{\lambda} \neq 1$ when looking at (3.13) and (3.18) all together. The leading term $(3\hat{\lambda})^{-1}$ in (3.20) also coincides with the leading contribution to (3.16) for $\hat{\lambda} \gg 1$, just like the case of oscillatory rotation in which the leading order result for $\hat{\delta} \ll 1$ coincides with that for $\hat{\lambda} \gg 1$. Since the steady torque for any value of $\hat{\lambda}$ will dominate for long time $t/t_\nu \gg 1$, we conclude that the steady torque for $\hat{\lambda} \gg 1$ will dominate the response for all time, as also shown for $\hat{\lambda} = 10$ in figure 3(*a*).

3.4. *Case of* $\hat{\lambda} = 1$

In the special case of $\hat{\lambda} = 1$, the torque takes a form similar to (3.7):

$$\frac{T_z(t)}{-8\pi\mu a^3} = \frac{1}{4}\left[\Omega(t) + \frac{1}{3}\int_0^t \frac{\mathrm{d}\Omega(t')}{\mathrm{d}t'}K_2(t-t')\,\mathrm{d}t'\right], \tag{3.21}$$

with the memory kernel K_2 different from (3.8):

$$K_2 = (1 + 8(t/t_\nu))\exp(4t/t_\nu)\mathrm{erfc}\left(2\sqrt{t/t_\nu}\right) - \frac{4}{\sqrt{\pi}}\sqrt{t/t_\nu}. \tag{3.22}$$

This memory kernel for $\hat{\lambda} = 1$ is new and exists only when slip is present.

For an impulsive rotation, equation (3.21) is reduced to

$$\frac{T_z(t)}{-8\pi\mu a^3} = \frac{1}{4}\left[1 + \frac{1}{3}K_2(t)\right]\Omega_0. \tag{3.23}$$

For short time $t/t_\nu \ll 1$, $K_2 = 1 - (8/\pi)\sqrt{t/t_\nu} + O(t/t_\nu)$. Although K_2 contributes to a constant at leading order, it is comparable to the steady torque part '1' in the bracket of (3.23). Evidently, because $\lambda = a$, the constant torque found for short time, $T_z\,(t \to 0) = -8\pi\mu a^3\Omega_0/3$, will start to decline at $t \sim t_\nu = a^2/\nu$. Also, together with (3.13) and (3.18), we find $T_z(t \to 0) = -8\pi\mu a^3\Omega_0/3\hat{\lambda}$ which coincides with the result for large $\hat{\lambda}$. This is because at a sufficiently small t the boundary layer is thin, and even if $\hat{\lambda}$ is small, the actual extent of slip is large.

4. Concluding remarks

To sum up, we have shown that a fraction of surface slip can dramatically change the characteristics of the history force on a spherical particle when undergoing an

unsteady motion. The changes can be revealed in the oscillatory translation of a slippery sphere (of radius a) and in particular manifest by the viscous force response in the high-frequency regime where slip effects are strong with the boundary layer thickness δ much thinner than the slip length λ. In this regime, we find two features very distinct from those for non-spherical and fluid particles reported previously (Lawrence & Weinbaum 1986; Yang & Leal 1991; Galindo & Gerbeth 1993): (i) the force saturation with a constant plateau of $O(a/\lambda)$ much greater than the steady drag and (ii) the persistence of the plateau until the SST point at $\delta \sim \lambda$, beyond which δ becomes thicker and the usual Basset response takes over. Similar features can also occur for the short-time force response for a slippery sphere subject to a sudden movement, as well as for the torque response when the sphere undergoes rotary oscillations. In addition, for translational and rotary oscillations, slip can further introduce a phase jump from the no-slip value to zero in the high-frequency limit. As these features always respond exclusively to λ no matter how small λ is, they can be used to extract the value of λ for a small particle and hence might provide a more convenient way to quantify the amount of surface slip of colloidal particles with experiments.

In practice, such experiments seem feasible by having particles propelled by acoustic forces under which the operating frequency ω typically ranges from 100 kHz to 10 MHz (Laurell, Petersson & Nilsson 2007). Let us take a micrometre-sized particle of $a \sim 1$ μm as an example. Suppose that one can manage to make the particle migrate in an oscillatory manner at a peak velocity $U_0 \sim 10$ μm s^{-1} in water of $\rho = 1$ g cm^{-3} and $\mu = 10^{-2}$ g cm^{-1} s^{-1}. This value for U_0 is chosen to ensure that the particle is moving under $Re = \rho U_0 a/\mu \ll 1$ (which requires $U_0 \ll 10^2$ cm s^{-1}) while keeping the Peclet number $Pe = U_0 a/D_p \gg 1$ (which requires $U_0 \gg 0.2$ μm s^{-1}) without being mitigated by Brownian motion, where $D_p = k_B T/6\pi\mu a$ (with $k_B T$ being the thermal energy, 4×10^{-21} J at 300 K) is the particle's diffusivity according to the Stokes–Einstein formula. At low ω below $\nu/2\pi a^2 \sim 10^5$ Hz, the particle will experience a Stokes drag $F_{Stokes} = 6\pi\mu U_0 a \sim 20$ pN. Suppose the slip length is merely 10 % of the particle radius, i.e. $\lambda \sim 100$ nm. One should observe a much larger force plateau $F_{plateau} = F_{Stokes}(a/\lambda) \sim 200$ pN (after subtracting the added mass) at ω higher than $\nu/2\pi\lambda^2 \sim 10^7$ Hz. Because the frequencies estimated above fall into the frequency range of typical ultrasound experiments and also because the forces here are detectable, it seems possible to extract the slip length of a colloidal particle with such experiments.

Acknowledgement

This work was supported by the Ministry of Science and Technology of Taiwan under grant MOST 107-2811-E-006-010 to H.-H.W.

Appendix A. Derivation of the general time-dependent force law (2.19)

In this appendix we derive the general force expression (2.19) for an arbitrary time-dependent translation of a slippery sphere. Expressing the particle velocity as a Fourier integral $U(t) = (2\pi)^{-1}\int_{-\infty}^{\infty} U(\omega)\mathrm{e}^{-\mathrm{i}\omega t}\,\mathrm{d}\omega$, we can transform (2.10) to

$$F(\omega) = -6\pi\mu U(\omega)a\left[\left(\frac{1+2\hat{\lambda}}{1+3\hat{\lambda}}\right)\left(\frac{1+\sqrt{2}\mathrm{e}^{-\mathrm{i}(\pi/4)}\dfrac{1}{\hat{\delta}}}{1+\dfrac{\hat{\lambda}}{1+3\hat{\lambda}}\sqrt{2}\mathrm{e}^{-\mathrm{i}(\pi/4)}\dfrac{1}{\hat{\delta}}}\right)+\frac{2}{9}\mathrm{e}^{-\mathrm{i}(\pi/2)}\frac{1}{\hat{\delta}^2}\right]. \quad \text{(A 1)}$$

With $e^{-i\pi/4} = -i^{1/2}$, $e^{-i\pi/2} = -i$ and $\hat{\delta} = (2\nu/\omega a^2)^{1/2}$, we first rewrite (A 1) as

$$F(\omega) = -6\pi\mu U(\omega) a \left[\left(\frac{1+2\hat{\lambda}}{1+3\hat{\lambda}} \right) \left(\frac{1 + \dfrac{-i^{1/2}\omega^{1/2}a}{\nu^{1/2}}}{1+\beta\dfrac{-i^{1/2}\omega^{1/2}a}{\nu^{1/2}}} \right) - \frac{2i}{9}\frac{\omega a^2}{2\nu} \right], \tag{A 2}$$

where $\beta = \hat{\lambda}/(1+3\hat{\lambda})$. The corresponding Laplace transform can be readily obtained by replacing $-i\omega$ with s. As we expect that its inverse will involve dU/dt and its convolution integral, it may be more convenient to express the Laplace transform of (A 2) as a product of $sU(s)$ and the remaining term:

$$\frac{F(s)}{-6\pi\mu a} = \left(\left(\frac{1+2\hat{\lambda}}{1+3\hat{\lambda}} \right) \left(\frac{1+t_\nu^{1/2}s^{1/2}}{1+\beta t_\nu^{1/2}s^{1/2}} \right) \left(\frac{1}{s} \right) + \frac{t_\nu}{9} \right) sU(s), \tag{A 3}$$

where $t_\nu = a^2/\nu$. Further rewriting (A 3) as

$$\frac{F(s)}{-6\pi\mu a} = \left(\left(\frac{1+2\hat{\lambda}}{1+3\hat{\lambda}} \right) \left(\frac{1}{s} + \frac{1-\beta}{\dfrac{s^{1/2}}{t_\nu^{1/2}} + s\beta} \right) + \frac{t_\nu}{9} \right) sU(s), \tag{A 4}$$

its inverse Laplace transform (denoted by $\mathcal{L}^{-1}$) is found to consist of three terms:

$$\begin{aligned} \frac{F(t)}{-6\pi\mu a} &= \left(\frac{1+2\hat{\lambda}}{1+3\hat{\lambda}} \right) \mathcal{L}^{-1}\{U(s)\} + \left(\frac{1+2\hat{\lambda}}{1+3\hat{\lambda}} \right) (1-\beta)\mathcal{L}^{-1}\left\{ \frac{1}{t_\nu^{-1/2}s^{1/2} + s\beta} sU(s) \right\} \\ &\quad + \frac{t_\nu}{9}\mathcal{L}^{-1}\{sU(s)\}. \end{aligned} \tag{A 5}$$

Assume that the particle starts from rest, i.e. $U = 0$ for $t < 0$ and $U = U(t)$ for $t \geqslant 0$. The inverse Laplace transforms in the first and last terms are simply $\mathcal{L}^{-1}\{U(s)\} = U(t)$ and $\mathcal{L}^{-1}\{sU(s)\} = dU/dt$. That in the second term essentially is a convolution integral $\int_0^t G(t-t')g(t')dt'$ of $g(t) = \mathcal{L}^{-1}\{sU(s)\} = dU/dt$ and the function from the following inverse Laplace transform:

$$G(t) = \mathcal{L}^{-1}\left\{ \frac{1}{t_\nu^{-1/2}s^{1/2} + \beta s} \right\} = \frac{1}{\beta}\exp(\beta^{-2}t/t_\nu)\operatorname{erfc}\left(\beta^{-1}\sqrt{t/t_\nu}\right). \tag{A 6}$$

Equation (A 6) is the memory kernel (2.20). With the inverse Laplace transforms given above, equation (A 5) can be readily reduced to (2.19).

Appendix B. Derivation of the general time-dependent torque expression from (3.6)

In this appendix we derive the torque expression for an arbitrary time-dependent torque rotation of a slippery sphere. We first take a Fourier transform for $\Omega(t)$ and write (3.2) in terms of $\Omega(\omega)$:

$$\frac{T_z(\omega)}{-8\pi\mu a^3} = \Omega(\omega)\frac{1 + \sqrt{2}e^{-i(\pi/4)}\dfrac{1}{\hat{\delta}} + \dfrac{2}{3}e^{-i(\pi/2)}\dfrac{1}{\hat{\delta}^2}}{1 + \sqrt{2}e^{-i(\pi/4)}\dfrac{1}{\hat{\delta}} + 3\hat{\lambda}\left[1 + \sqrt{2}e^{-i(\pi/4)}\dfrac{1}{\hat{\delta}} + \dfrac{2}{3}e^{-i(\pi/2)}\dfrac{1}{\hat{\delta}^2}\right]}. \tag{B 1}$$

Similar to (A 3), the Laplace transform converted from (B 1) can be rewritten as

$$\frac{T_z(s)}{-8\pi\mu a^3} = \frac{1}{1+3\hat{\lambda}}\left(\frac{1}{s}+Q(s)\right)s\Omega(s), \tag{B 2}$$

where

$$Q(s) = \frac{t_\nu/3}{(1+3\hat{\lambda})(1+t_\nu^{1/2}s^{1/2})+\hat{\lambda}t_\nu s}. \tag{B 3}$$

Assume that $\Omega = 0$ for $t < 0$ and $\Omega = \Omega(t)$ for $t \geqslant 0$. The inverse Laplace transform of (B 2) can be readily determined as

$$\frac{T_z(t)}{-8\pi\mu a^3} = \frac{1}{1+3\hat{\lambda}}[\Omega(t)+\mathcal{L}^{-1}\{Q(s)s\Omega(s)\}], \tag{B 4}$$

in which the inverse Laplace transform of the second term on the right-hand side can be expressed as a convolution integral:

$$\mathcal{L}^{-1}\{Q(s)s\Omega(s)\} = \int_0^t Q(t-t')\frac{\mathrm{d}\Omega(t')}{\mathrm{d}t'}\,\mathrm{d}t'. \tag{B 5}$$

The remaining task is to determine $Q(t)$ from $\mathcal{L}^{-1}\{Q(s)\}$.

First consider $\hat{\lambda} = 0$. Equation (B 3) is reduced to

$$Q(s) = \frac{t_\nu^{1/2}}{3(t_\nu^{-1/2}+s^{1/2})}. \tag{B 6}$$

Using

$$\mathcal{L}^{-1}\left\{\frac{1}{s^{1/2}+\alpha}\right\} = -\alpha\mathrm{erfc}\left(\alpha\sqrt{t}\right)\exp(\alpha^2 t)+\frac{1}{\sqrt{t\pi}}, \tag{B 7}$$

the inverse Laplace transform of (B 6) is given by

$$Q(t) = \frac{1}{3}\left(-\mathrm{erfc}\left(\sqrt{t/t_\nu}\right)\exp(t/t_\nu)+\frac{1}{\sqrt{\pi}}\sqrt{\frac{t_\nu}{t}}\right). \tag{B 8}$$

Subsituting (B 8) into (B 5) in (B 4) gives (3.7) with the memory kernel (3.8).

For $0 < \hat{\lambda} < 1$, equation (B 3) can be rewritten as

$$Q(s) = \frac{t_\nu^{1/2}}{3xy}\left(\frac{1}{s^{1/2}+\dfrac{x}{2t_\nu^{1/2}\hat{\lambda}}[x-y]}+\frac{1}{s^{1/2}+\dfrac{x}{2t_\nu^{1/2}\hat{\lambda}}[x+y]}\right), \tag{B 9}$$

with $x = \sqrt{1+3\hat{\lambda}}$ and $y = \sqrt{|1-\hat{\lambda}|}$. Using (B 7), we find the inverse Laplace transform of (B 9) to be

$$Q(t) = (3y)^{-1}[-E_1(x,-y)+E_1(x,y)], \tag{B 10}$$

where

$$E_1(x,y) = (x+y)/2\hat{\lambda}\times\exp((x^2/2\hat{\lambda}^2)((1+\hat{\lambda})+xy)t/t_\nu)\mathrm{erfc}\left((x/2\hat{\lambda})(x+y)\sqrt{t/t_\nu}\right). \tag{B 11}$$

Equation (B 10) gives the kernel function (3.12), leading to (3.11) after substitution of (B 10) into (B 5) in (B 4).

For $\hat{\lambda} > 1$, (B 9) is changed to

$$Q(s) = \frac{t_v^{1/2}}{3xyi}\left(\frac{1}{s^{1/2} + \dfrac{x}{2t_v^{1/2}\hat{\lambda}}[x - \mathrm{i}y]} - \frac{1}{s^{1/2} + \dfrac{x}{2t_v^{1/2}\hat{\lambda}}[x + \mathrm{i}y]}\right). \tag{B 12}$$

Using (B 7), the corresponding inverse Laplace transform can be determined as

$$Q(t) = (3\mathrm{i}y)^{-1}[-E_2(x, -y) + E_2(x, y)], \tag{B 13}$$

where

$$E_2(x, y) = (x + \mathrm{i}y)/2\hat{\lambda} \times \exp((x^2/2\hat{\lambda}^2)((1 + \hat{\lambda}) + \mathrm{i}xy)t/t_v)\mathrm{erfc}\left((x/2\hat{\lambda})(x + \mathrm{i}y)\sqrt{t/t_v}\right). \tag{B 14}$$

Substituting (B 13) into (B 4) in (B 5), we can obtain (3.16) with the memory kernel (3.17).

In the special case of $\hat{\lambda} = 1$, equation (B 3) is reduced to

$$Q(s) = \frac{1}{3\left(s^{1/2} + \dfrac{2}{t_v^{1/2}}\right)^2}. \tag{B 15}$$

Making use of

$$\mathcal{L}^{-1}\left\{\frac{1}{(s^{1/2} + \alpha)^2}\right\} = (1 + 2\alpha^2 t)\exp(\alpha^2 t)\mathrm{erfc}\left(\alpha\sqrt{t}\right) - 2\alpha\sqrt{\frac{t}{\pi}}, \tag{B 16}$$

the inverse Laplace transform of (B 15) can be found to be

$$Q(t) = \frac{1}{3}(1 + 8(t/t_v))\exp(4t/t_v)\mathrm{erfc}\left(2\sqrt{t/t_v}\right) - \frac{4}{\sqrt{\pi}}\sqrt{t/t_v}. \tag{B 17}$$

The torque expression (3.21) with the memory kernel (3.22) can then be obtained after substituting (B 17) into (B 5) in (B 4).

REFERENCES

ALBANO, A. M., BEDEAUX, D. & MAZUR, P. 1975 On the motion of a sphere with arbitrary slip in a viscous incompressible fluid. *Physica* A **80**, 89–97.

ASHMAWY, E. A. 2012 Unsteady rotational motion of a slip spherical particle in a viscous fluid. *ISRN Math. Phys.* **2012**, 513717.

ASHMAWY, E. A. 2017 Unsteady translational motion of a slip sphere in a viscous fluid using the fractional Navier–Stokes equation. *Eur. Phys. J. Plus* **132** (3), 142.

BASSET, A. B. 1888 On the motion of a sphere in a viscous liquid. *Phil. Trans. R. Soc. Lond.* A **179**, 43–63.

BENTWICH, M. & MILOH, T. 1978 The unsteady matched Stokes–Oseen solution for the flow past a sphere. *J. Fluid Mech.* **88**, 17–32.

FELDERHOF, B. U. 1976 Force density induced on a sphere in linear hydrodynamics: II. Moving sphere, mixed boundary conditions. *Physica* A **84**, 569–576.

FENG, J. & JOSEPH, D. D. 1995 The unsteady motion of solid bodies in creeping flows. *J. Fluid Mech.* **303**, 83–102.

FUJIOKA, H. & WEI, H.-H. 2018 Letter: new boundary layer structures due to strong wall slippage. *Phys. Fluids* **30** (12), 121702.

GALINDO, V. & GERBETH, G. 1993 A note on the force on an accelerating spherical drop at low-Reynolds number. *Phys. Fluids* A **5**, 3290–3292.

GARBIN, V., DOLLET, B., OVERVELDE, M., COJOC, D., DI FABRIZIO, E., VAN WIJNGAARDEN, L., PROSPERETTI, A., DE JONG, N., LOHSE, D. & VERSLUIS, M. 2009 History force on coated microbubbles propelled by ultrasound. *Phys. Fluids* **21** (9), 092003.

GATIGNOL, R. 2007 On the history term of Boussinesq–Basset when the viscous fluid slips on the particle. *C. R. Méc.* **335**, 606–616.

KIM, S. & KARRILA, S. J. 1991 *Microhydrodynamics: Principles and Selected Applications*. Butterworth–Heinemann.

LANDAU, L. D. & LIFSHITZ, E. M. 1987 *Fluid Mechanics*. Pergamon.

LAURELL, T., PETERSSON, F. & NILSSON, A. 2007 Chip integrated strategies for acoustic separation and manipulation of cells and particles. *Chem. Soc. Rev.* **36** (3), 492–506.

LAWRENCE, C. J. & WEINBAUM, S. 1986 The force on an axisymmetric body in linearized, time-dependent motion: a new memory term. *J. Fluid Mech.* **171**, 209–218.

LAWRENCE, C. J. & WEINBAUM, S. 1988 The unsteady force on a body at low Reynolds number: the axisymmetric motion of a spheroid. *J. Fluid Mech.* **189**, 463–489.

LOVALENTI, P. M. & BRADY, J. F. 1993 The force on a bubble, drop, or particle in arbitrary time-dependent motion at small Reynolds number. *Phys. Fluids* A **5** (9), 2104–2116.

MAGNAUDET, J. & LEGENDRE, D. 1998 The viscous drag force on a spherical bubble with a time-dependent radius. *Phys. Fluids* **10** (3), 550–554.

MICHAELIDES, E. E. & FENG, Z. G. 1995 The equation of motion of a small viscous sphere in an unsteady flow with interface slip. *Intl J. Multiphase Flow* **21**, 315–321.

POZRIKIDIS, C. 1989 A singularity method for unsteady linearized flow. *Phys. Fluids* A **1**, 1508–1520.

SIMHA, A., MO, J. & MORRISON, P. J. 2018 Unsteady Stokes flow near boundaries: the point-particle approximation and the method of reflections. *J. Fluid Mech.* **841**, 883–924.

TAKEMURA, F. & MAGNAUDET, J. 2004 The history force on a rapidly shrinking bubble rising at finite Reynolds number. *Phys. Fluids* **16** (9), 3247–3255.

WANG, S. & ARDEKANI, A. M. 2012 Unsteady swimming of small organisms. *J. Fluid Mech.* **702**, 286–297.

YANG, S. M. & LEAL, L. G. 1991 A note on memory-integral contributions to the force on an accelerating spherical drop at low Reynolds number. *Phys. Fluids* A **3**, 1822–1824.

YIH, C.-S. 1977 *Fluid Mechanics: A Concise Introduction to the Theory*. West River Press.

ZHANG, W. & STONE, H. A. 1998 Oscillatory motions of circular disks and nearly spherical particles in viscous flows. *J. Fluid Mech.* **367**, 329–358.